

## INTERSTELLAR INTERFEROMETRY OF THE PULSAR PSR 1237 + 25

A. WOLSZCZAN

National Astronomy and Ionosphere Center, Cornell University

AND

J. M. CORDES<sup>1</sup>

Astronomy Department and National Astronomy and Ionosphere Center, Cornell University;  
 and Astronomy Department, California Institute of Technology

*Received 1987 April 28; accepted 1987 June 12*

### ABSTRACT

An episode of exceptionally prominent double imaging of the pulsar PSR 1237 + 25 caused by refraction in the interstellar medium has been detected with the Arecibo telescope at 430 MHz and used to resolve the pulsar magnetosphere for the first time. Multiple imaging causes quasi-periodic modulation of the pulsar intensity in time and frequency that represents the fringe pattern of an “interstellar interferometer” with a baseline of the order of 1 AU. Assuming that refraction occurred midway between the pulsar and the observer, the separation of images of PSR 1237 + 25 was  $\sim 3.3$  mas and the effective baseline of our interferometer was  $\sim 1$  AU corresponding to an angular resolution of  $\sim 1$  micro-arcsec. From the detected fringe phase shift across the pulse profile of PSR 1237 + 25, we have estimated a typical transverse separation between the emitting regions to be  $\sim 10^8$  cm. This estimate depends on the assumed distance to the refracting region and may be much smaller. We show that the observed fringe shifts and their dependence on pulse phase are inconsistent with a simple magnetic dipole model of pulsar emission.

*Subject headings:* interstellar: matter — interferometry — pulsars

### I. INTRODUCTION

Recent observations have shown that refraction can significantly modify the interstellar scintillation (ISS) patterns arising from diffractive scatter of pulsar signals propagating through the interstellar medium (Roberts and Ables 1982; Hewish, Wolszczan, and Graham 1985; Cordes and Wolszczan 1986). Refraction effects also underlie at least part of the low-frequency variability of pulsars and compact extragalactic radio sources (e.g., Rickett, Coles, and Bourgois 1984; Rickett 1986; Romani, Narayan, and Blandford 1986). In their most dramatic form, refraction from discrete structures in the interstellar medium yields caustics that appear as intensity spikes and are superposed with an intensity trough (Fiedler *et al.* 1987).

Strong refraction events can split the apparent source image into two or more distinct subimages. For pulsars, the resultant dynamic spectra (intensity as a function of time and frequency) are the superposition of separate patterns from each subimage combined with oscillatory cross terms caused by beating between subimages (Cordes and Wolszczan 1986). The oscillatory terms are equivalent to fringes obtained with an interferometer baseline  $\sim 1$  AU, sufficiently large to potentially resolve the pulsar magnetosphere (Cordes, Pidwerbetsky, and Lovelace 1986). Episodes of refractive multiple imaging may lead to higher spatial resolution than diffractive scintillations alone, because fringe spacings are often substantially less than the widths of diffraction features. Previous attempts to resolve

the magnetosphere using diffractive scintillations have provided upper limits on the separations of pulsar emission regions (Cordes, Weisberg, and Boriakoff 1983).

In this *Letter*, we report an exceptionally prominent multiple imaging event of the pulsar PSR 1237 + 25, most probably caused by a discrete structure located significantly nearer the pulsar than Earth. From an analysis of dynamic spectra, we demonstrate that the transverse separations of emission regions in the pulsar magnetosphere are large enough to be resolved by the “interstellar interferometer.” We discuss the implications of our results for models of the pulsar magnetosphere. We also suggest that the refracting structure is similar in kind to those that cause dramatic focusing effects in the light curves of compact extragalactic radio sources (Fiedler *et al.* 1987).

### II. OBSERVATIONS

Measurements of dynamic spectra of PSR 1237 + 25 were made on 1986 December 9, 22, and 28 at 430 MHz with the Arecibo radiotelescope and the three-level, 40 MHz correlation spectrometer. The 512 lag autocorrelation functions of the two circularly polarized input signals were integrated in 128 pulse phase bins for 10 s, synchronously with the Doppler-corrected pulsar period. Each set of  $2 \times 128$  integrated correlation functions was then written to a magnetic tape for further processing. The total observing time per day varied from 30 to 40 minutes. “Off-line” processing included correction of the correlation functions for three-level sampling followed by the computation of spectra integrated over

<sup>1</sup>Alfred P. Sloan Foundation Fellow.

a predefined “on-pulse” window and normalized with respect to the spectra accumulated in “off-pulse” phase bins. The normalized 10 MHz spectra had a resolution of 19.5 kHz, and the effective time interval between spectra, which included the integration and the tape I/O time, was 19 s. Phase bins were separated by 11 ms or 2°8 of longitude (where 360° of longitude corresponds to one pulse period). With this resolution, the pulse waveform of width  $\sim 18^\circ$  was resolved although the five individual pulse components (e.g., Backer 1970), separated by about  $3^\circ$ , were unresolved.

### III. DYNAMIC SPECTRA

In Figure 1a (Plate L2), we show dynamic spectra obtained by integrating over the entire pulse window (to obtain the best signal-to-noise ratio). They display a strikingly periodic intensity modulation as a function of time and frequency for the first two epochs. On December 28, however, broad amorphous features are dominant.

We are convinced that all modulations are caused by propagation in the interstellar medium, rather than being instrumental in origin or intrinsic to the pulsar. First of all, the spectra of the pulsar PSR 1133+16 taken on the same days with identical observing parameters appeared similar to those obtained at previous times (e.g., Hewish, Wolszczan, and Graham 1985; Cordes, Weisberg, and Boriakoff 1983; Cordes and Wolszczan 1986) and were markedly different from the spectra of PSR 1237+25. Moreover, the dynamic spectrum of December 28 is typical of those observed while monitoring PSR 1237+25 over the course of a year (unpublished data). Finally, similar but less dramatic oscillations are seen at some epochs for other objects and have parameters that scale strongly with radio frequency and with pulsar distance, as is expected, if they are due to propagation through a cold turbulent plasma.

A simple model suffices to explain the scintillation features seen in dynamic spectra (Cordes and Wolszczan 1986 and references therein). Recent work suggests that refraction from discrete structures in the interstellar medium may dominate refraction from distributed turbulence, so a thin screen model may be appropriate. Therefore, our model consists of a thin screen in which refractive phase variations  $\phi_r$  (defined as those produced on length scales larger than the Fresnel scale  $[\lambda D_s(1 - D_s/D)]^{1/2}$ , where  $\lambda$  is the wavelength,  $D$  is the distance from Earth to the pulsar, and  $D_s$  is the pulsar-screen distance) give rise to a pair of subimages of the pulsar, each of which is diffracted by scales smaller than the Fresnel scale into an observed size  $\theta_d$ . For simplicity, we assume that diffraction arises from electron density fluctuations throughout the line of sight, because diffraction effects seem to occur at all epochs. Of course, the refracting screen may also contain small-scale structure that contributes to the diffraction. Since the analysis below is not particularly sensitive to our assumptions about the diffraction, we assume that it is not overly modified by the refracting screen.

In our model, each subimage leads to time and frequency structure with characteristic scales  $\Delta t_d \approx \lambda/2\pi\theta_d V_\perp$  and  $\Delta\nu_d \approx c/\pi(D - D_s)\theta_d^2$ , where  $V_\perp$  is the transverse velocity. The intensity of each image is the pulsar intensity times a “gain” (magnification) determined by phase curvature (Cordes,

TABLE 1  
MEASURED ISS PARAMETERS FOR PSR 1237+25

Date (1986)	$\Delta\nu_d$ (kHz)	$\Delta t_d$ (s)	$P_v$ (kHz)	$P_t$ (s)	$\theta_d$ (mas)	$\theta_{\text{split}}$ (mas)
Dec 9.....	442	146	313	1380	1.0	3.3
Dec 22.....	615	260	667	1260	0.8	2.2
Dec 28.....	817	244	...	...	0.7	...

Pidwerbetsky, and Lovelace 1986, eq. [12]). The net dynamic spectrum is the incoherent sum of two independent dynamic spectra combined with an oscillating cross term whose phase  $\Phi$  is simply due to the geometrical path length difference between the two subimages. The oscillation period in frequency,  $P_v = 2\pi/|d\Phi/d\nu|$ , is

$$P_v = \frac{2cD}{3D_s(D - D_s)(\theta_2^2 - \theta_1^2)} \approx 0.28 [D_s (\text{kpc}) (1 - D_s/D)(\theta_2^2 - \theta_1^2)_{\text{mas}}]^{-1} \text{ MHz}, \quad (1)$$

where  $\theta_{1,2}$  are the refraction angles (at the screen) of the two images. A similar period,  $P_t$  along the time axis, may also be derived (Cordes and Wolszczan 1986), but we are not concerned with it here.

To quantify the structure in the dynamic spectra we performed several correlation and power spectrum analyses, as discussed in Cordes and Wolszczan (1986). In Table 1 we give empirical parameters such as the diffraction bandwidth  $\Delta\nu_d$ , diffraction time scale  $\Delta t_d$ , oscillation periods  $P_v$  and  $P_t$  and derived angles,  $\theta_d \approx (c/\pi D \Delta\nu_d)^{1/2}$  (the diffraction angle), and the splitting angle  $\theta_{\text{split}} = (\theta_2^2 - \theta_1^2)^{1/2}$  estimated from  $P_v$ , assuming a pulsar distance of 0.33 kpc (Manchester and Taylor 1981). We have assumed  $D_s = D/2$  to obtain values for the table.

Figure 1b shows two-dimensional fluctuation spectra of the ISS patterns of Figure 1a. Coordinate axes are fluctuation frequencies that are reciprocals to the periods  $P_v$  and  $P_t$ . The fluctuation spectra are inversion symmetric about the origin. Peaks in the spectra near the origin are due to the diffractive scintillations and are always expected to appear, while “out-riders” components associated with beating between subimages are ephemeral. Distance from the origin of outriders increases with larger image splitting angles. For both December 9 and December 22, the source image is predominantly double, although on the latter date the image may also contain two additional subimages.

The entire episode of refractive imaging certainly lasted longer than our observing period of  $T = 19$  days. Since the transverse velocity of PSR 1237+25,  $V_\perp \approx 178 \text{ km s}^{-1}$  (Lyne, Anderson, and Salter 1982), must dominate the net drift velocity of the ISS pattern of this pulsar, we can derive a lower limit to the spatial scale of the observed refractive process,  $V_\perp T = 3 \times 10^{13} \text{ cm}$ , which is within the range of scale sizes assumed to cause refractive scintillation phenomena (Rickett 1986).

PLATE L2

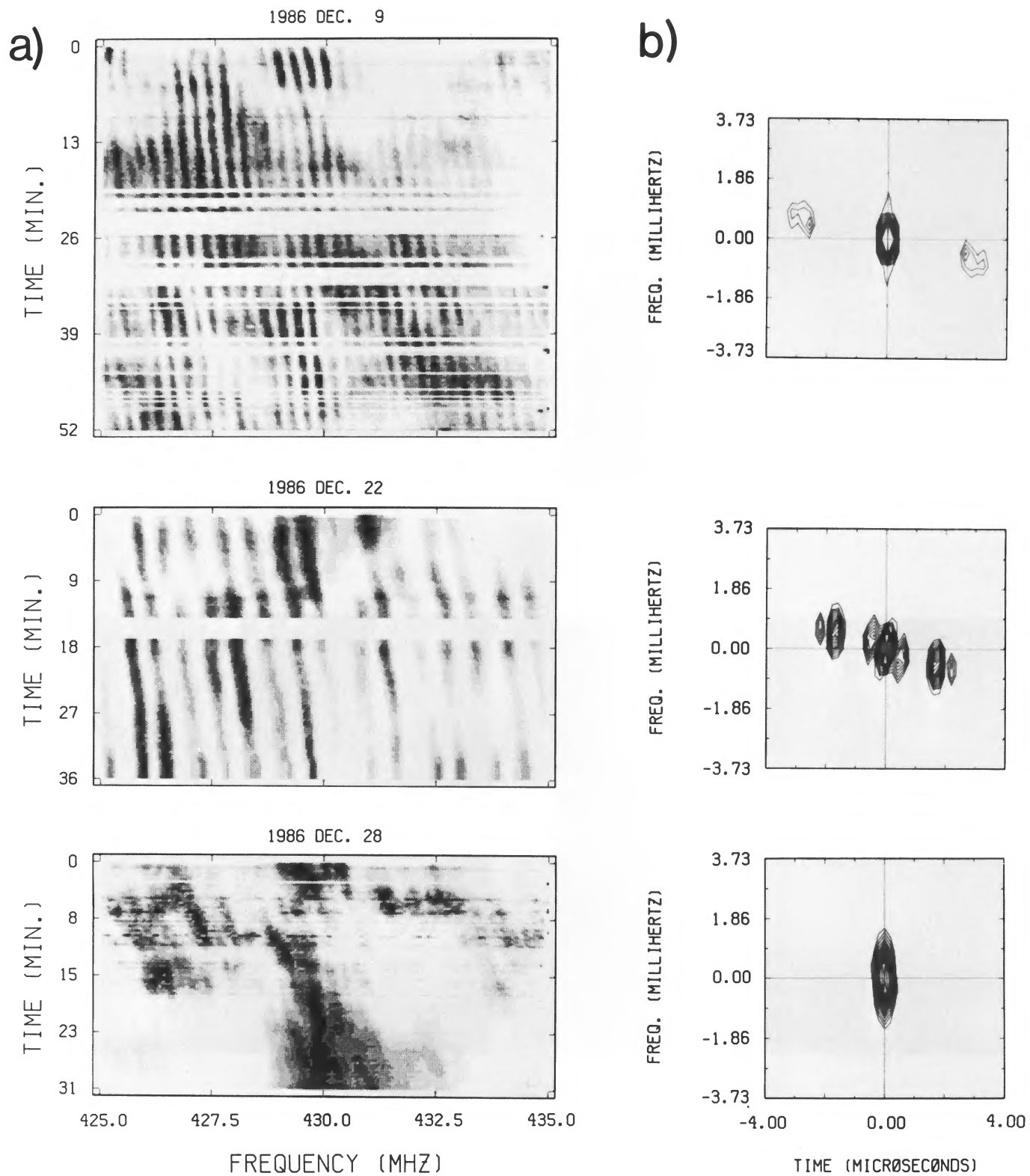


FIG. 1.—(a) Dynamic spectra of PSR 1237+25 at three epochs and (b) their two-dimensional fluctuation spectra. Blank lines in the dynamic spectra denote the data rejected due to interference.

WOLSCZAN AND CORDES (see 320, L36)

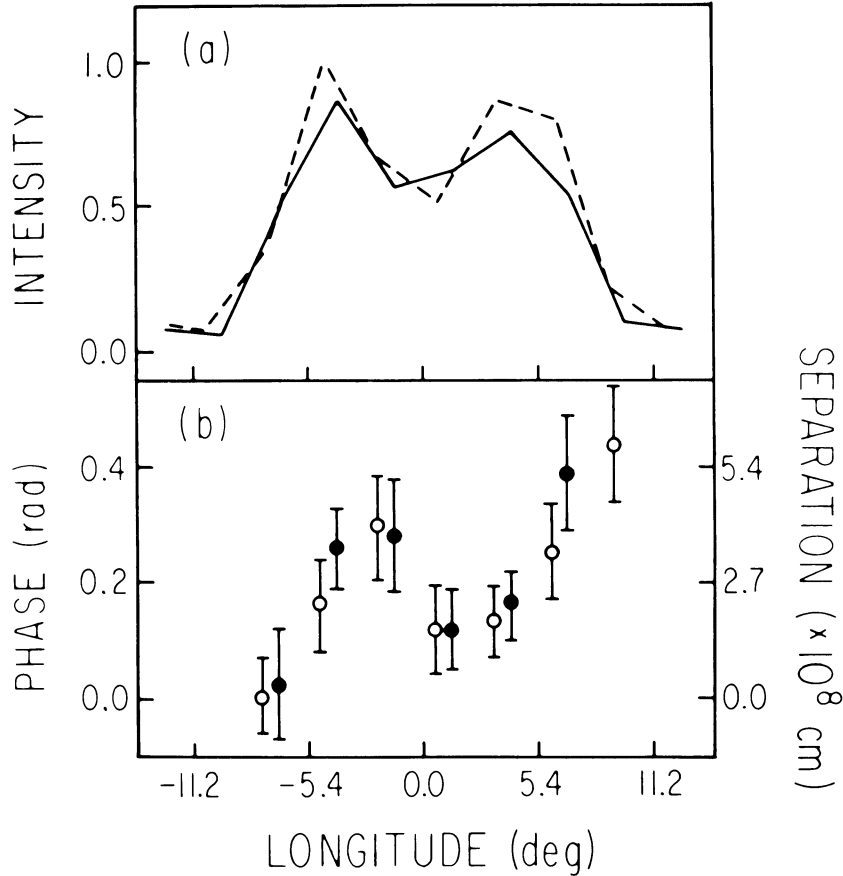


FIG. 2.—(a) Integrated pulse profiles of PSR 1237+25 obtained on December 9 (*solid line*) and December 22 (*dashed line*). (b) Fringe phases measured with respect to the phase at the leading edge of the pulse profile for dynamic spectra of December 9 (*filled circles*) and December 22 (*open circles*). The December 22 phases are scaled and shifted in longitude as explained in the text.

#### IV. RESOLVING THE PULSAR MAGNETOSPHERE

As with any interference pattern, transverse displacement of a radio source by a distance  $\delta x_s$  induces a phase shift. For our one-dimensional model, the phase shift is given by

$$\delta\phi = k\delta x_s(1 - D_s/D)[(G_2 - 1)\theta_2 - (G_1 - 1)\theta_1], \quad (2)$$

where  $k = 2\pi/\lambda$  and  $G_{1,2}$  are the gains associated with the two images. Equation (2) improves on the approximate expression given by equation (76) of Cordes, Pidwerbetsky, and Lovelace (1986). Gain variations as large as 100% are caused by refraction in the interstellar medium (e.g., Coles *et al.* 1987). Unfortunately, we are unable to determine the gains  $G_{1,2}$  directly from our data. Therefore we approximate the bracketed term as  $\zeta(\theta_2^2 - \theta_1^2)^{1/2}$ , where  $\zeta \approx 1$ , and obtain

$$\delta\phi \approx 0.053\zeta\nu_{\text{GHz}} \left( \frac{\delta x_s}{10^8 \text{ cm}} \right) \left[ \frac{D/D_s - 1}{D \text{ (kpc)} P_\nu \text{ (MHz)}} \right]^{1/2} \text{ rad.} \quad (3)$$

This phase shift will also be measured between the oscillation patterns seen from two radio sources separated by distance  $\delta x_s$ .

For the case of pulsars, from which relativistically beamed radiation is clearly controlled by an ambient magnetic field, it is likely that different pulse components are emitted from locations that are separated in the transverse direction (e.g., Fig. 5 of Cordes, Weisberg, and Boriakoff 1983). Consequently, we measured the fringe phase at different pulse longitudes to see if the pulsar magnetosphere had, in fact, been resolved during the multiple imaging event. Dynamic spectra were computed for 13 longitude bins within the pulse profile (Fig. 2a) using the data taken on December 9 and 22. The fringe phase difference was calculated by using the pulse longitude bin at the leading edge of the pulse as a reference. By cross correlating dynamic spectra for each longitude bin with those of the reference bin, we calculated the fringe phase as a function of pulse longitude. Figure 3 shows a representative cross correlation function in which the offset from zero lag is evident.

We combined the results from the two epochs showing oscillations according to the following considerations. The observed fringe displacement is proportional to  $P_\nu^{-1/2}$ . Therefore, if phase shifts derived from dynamic spectra having two different modulation periods  $P_{\nu 1}$  and  $P_{\nu 2}$  (at two epochs) are to be compared, a scaling factor  $(P_{\nu 2}/P_{\nu 1})^{1/2}$  must be applied to one set of phases. A composite phase difference curve with

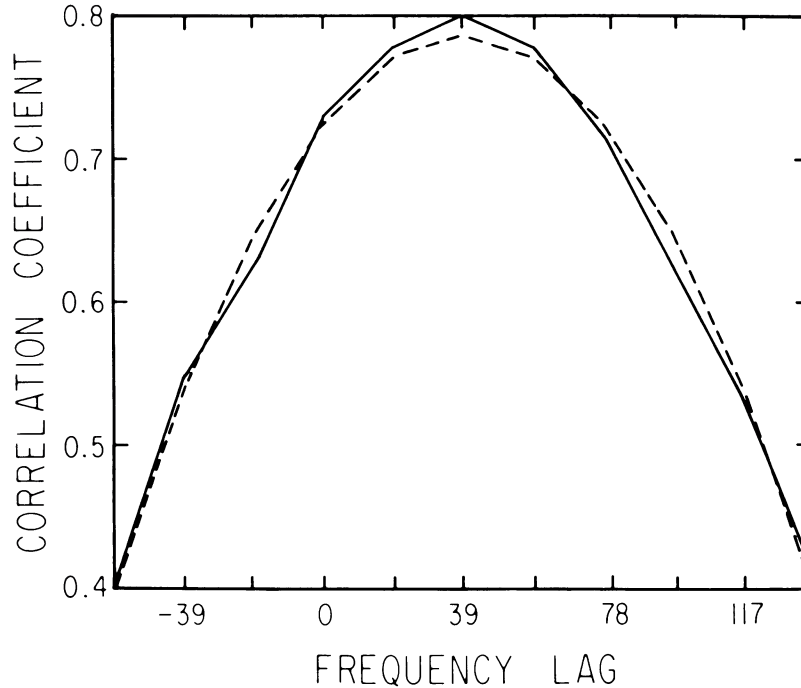


FIG. 3.—A frequency cross-correlation function (CCF) of the dynamic spectra measured at the opposite edges of the pulse profile (*solid line*) and a parabolic least-squares fit to the CCF (*dashed line*) used to determine the fringe phase shift.

appropriately scaled 22 December phases is shown in Figure 2*b*. In order to align pulse profiles, the December 22 profile has been shifted by  $0^{\circ}.7$  toward earlier longitudes.

The fringe phase varies smoothly over the pulse profile and is clearly antisymmetric about the profile center. The phase variations significantly exceed experimental errors and the fringe phases from the two epochs agree with each other extremely well. This not only adds to the reliability of our analysis but it also confirms the validity of the assumed model of refractive scintillation, via the scaling of the fringe phases as  $P_v^{-1/2}$ . The fringe phases computed separately for the two hands of circular polarization also agree within the errors. Moreover, fringe phases of another pulsar, PSR 0940+16, which has a similar dispersion measure to that of 1237+25, showed no variation with pulse longitude during an epoch of weak oscillations in the dynamic spectra. These results provide additional evidence that the fringe phase variations are determined by interstellar path length differences rather than being induced by instrumental effects.

With equation (3) the fringe phase may be used to estimate the spatial separation of the emission regions, as indicated on the right hand side of Figure 2*b*. The derived transverse separations vary between  $7 \times 10^7$  and  $6 \times 10^8$  cm (if the refracting screen is midway between Earth and pulsar). These separations are less than 10% of the light cylinder radius  $r_{LC} \equiv cP/2\pi = 10^{9.8}$  cm, where  $P$  is the pulsar period. To our knowledge, this is the first direct measurement of the spatial separation between the emission regions of a pulsar.

#### V. DISCUSSION

Our measurements indicate that the emission regions for PSR 1237+25 were resolved by the interference patterns seen

in 1986 December. Assuming strong relativistic beaming from particles with Lorentz factors  $\gamma > 100$  (e.g., Cheng and Ruderman 1979), we may conclude that pulse longitudes having the same fringe phase are emitted from the same angular position on the sky. Varying fringe phase shifts then indicate different angular positions which, in turn, imply differences in the product  $\delta x_s [(D/D_s - 1)/D]$  as a function of pulse longitude.

For a specific model of the magnetosphere, it is possible to relate  $\delta x_s$  to the altitude of emission. Assuming a dipolar magnetic field and emission at a constant altitude  $r_{em}$ ,  $\delta x_s \approx r_{em} \psi/3$ , where  $\psi$  is pulse longitude measured with respect to the pulse centroid, which corresponds to coplanarity of the line of sight, the dipole axis, and the spin axis of the pulsar; this expression holds so long as  $r_{em} \ll r_{LC}$  (e.g., Fig. 5 of Cordes, Weisberg and Boriakoff 1983). Using this model, we predict that the fringe phase should be *antisymmetric* with respect to  $\psi = 0$  and that it should vary monotonically. The measured fringe phase is asymmetric but is nonmonotonic. Moreover, the typical fringe phase difference of 0.2 rad implies (using parameters for PSR 1237+25)

$$\frac{r_{em}}{r_{LC}} \approx \frac{7}{\psi(\text{deg})(D/D_s - 1)^{1/2}}. \quad (4)$$

For  $\psi \approx 7^\circ$ , emission altitudes equal to the light cylinder radius are implied for a refracting screen that is midway,  $D = 2D_s$ .

Since arguments can be made on the basis of pulse shapes and polarization that emission altitudes are likely to be much smaller than the light cylinder radius, it may be necessary to

conclude that the refracting screen is much nearer the pulsar than Earth,  $D \gg D_s$ . For example,  $r_{\text{em}} = 0.1r_{\text{LC}}$  requires the screen distance from the pulsar to be only 1% of the pulsar-Earth distance, or about 3 pc. Alternatively, the magnetic field of PSR 1237+25 may deviate strongly from a dipolar form in the emission region and emission altitudes may vary such that transverse separations are much larger for a given pulse longitude than implied by the dipole model. This latter interpretation would also be consistent with the fact that the fringe phase vs. pulse longitude disagrees with a simple dipole model. We will leave it to future work, including ISS measurements with better pulse longitude resolution and further modeling, to interpret the fringe phase curve. We anticipate that polarization measurements, which are also sensitive to the magnetic field topology, will aid in the modeling.

In addition to resolving the pulsar magnetosphere, our measurements suggest that a discrete refracting structure of size  $> 1$  AU crossed the line of sight, producing a predominantly double image of the pulsar with a splitting angle between subimages of about  $2.3(1 - D_s/D)^{-1/2}$  mas at 0.43 GHz. This episode may be similar in origin to recent caustic events seen in the light curves of compact extragalactic radio sources (Fiedler *et al.* 1987), which suggest double imaging with splitting angles of a few mas at 2.7 GHz caused by a

discrete galactic structure. These have been interpreted (Romani, Blandford, and Cordes 1987) as sheetlike structures with an aspect ratio  $\sim 100$ , whereby edge-on events are associated with the extragalactic source events, and face-on events underlie oscillation episodes seen in pulsar dynamic spectra. The event seen here for PSR 1237+25 is described by a splitting angle consistent with a face-on event so long as there is structure across the sheet of order the sheet thickness, which would be at least a few AU. It is also possible that the ISM is filled with refracting structures of a wide variety of shapes and sizes. Clearly, much more work is needed to constrain the distribution of refracting structures.

We thank D. Backer, R. Blandford, and R. Romani for useful discussions and Shri Kulkarni and Phil Perillat for conceptualizing and writing the data acquisition software. This work was supported by the Alfred P. Sloan Foundation, by the National Science Foundation through grant 85-20530 to Cornell University, and by the National Astronomy and Ionosphere Center at Cornell which operates the Arecibo Observatory under contract to the National Science Foundation. This work was also supported by the Owens Valley Radio Observatory.

## REFERENCES

- Backer, D. C. 1970, *Nature*, **228**, 1297.  
 Cheng, A., and Ruderman, M. A. 1979, *Ap. J.*, **229**, 348.  
 Coles, W. A., Frehlich, R. G., Rickett, B. J., and Codona, J. L. 1987, *Ap. J.*, **315**, 666.  
 Cordes, J. M., Pidwerbetsky, A., and Lovelace, R. V. E. 1986, *Ap. J.*, **310**, 737.  
 Cordes, J. M., Weisberg, J. M., and Boriakoff, V. 1983, *Ap. J.*, **268**, 370.  
 Cordes, J. M., and Wolszczan, A. 1986, *Ap. J. (Letters)*, **307**, L27.  
 Fiedler, R. L., Dennison, B., Johnston, K. J., and Hewish, A. 1987, *Nature*, **326**, 675.  
 Hewish, A., Wolszczan, A., and Graham, D. A. 1985, *M.N.R.A.S.*, **192**, 799.  
 Lyne, A. G., Anderson, B., and Salter, C. J. 1982, *M.N.R.A.S.*, **201**, 503.  
 Manchester, R. N., and Taylor, J. H. 1981, *A.J.*, **86**, 1953.  
 Rickett, B. J. 1977, *Ann. Rev. Astr. Ap.*, **15**, 479.  
 ———. 1986, *Ap. J.*, **307**, 564.  
 Rickett, B. J., Coles, W. A., and Bourgois, G. 1984, *Astr. Ap.*, **134**, 390.  
 Roberts, J. A., and Ables, J. G. 1982, *M.N.R.A.S.*, **201**, 1119.  
 Romani, R. W., Blandford, R. D., and Cordes, J. M. 1987, *Nature*, submitted.  
 Romani, R., Narayan, R., and Blandford, R. 1986, *M.N.R.A.S.*, **220**, 19.

JAMES M. CORDES: Astronomy Department, Space Sciences Building, Cornell University, Ithaca, NY 14853

ALEXANDER WOLSZCZAN: National Astronomy and Ionosphere Center, Arecibo Observatory, Box 995, Arecibo, PR 00613